AD_____

Award Number: W81XWH-06-1-0315

TITLE: Revealing the Functions of Tenascin-C in 3-D Breast Cancer Models Using Cell Biological and In Silico Approaches

PRINCIPAL INVESTIGATOR: Agne Taraseviciute
Peter Lloyd Jones, Ph.D.

CONTRACTING ORGANIZATION: University of Pennsylvania
Philadelphia, PA 19104

REPORT DATE: March 2007

TYPE OF REPORT: Annual Summary

PREPARED FOR: U.S. Army Medical Research and Materiel Command
Fort Detrick, Maryland 21702-5012

REPORT DOCUMENTATION PAGE

Form Approved
OMB No. 0704-0188

1. REPORT DATE	2. REPORT TYPE	3. DATES COVERED
01-03-2007	Annual Summary	15 Feb 2006 – 14 Feb 2007

4. TITLE AND SUBTITLE

Revealing the Functions of Tenascin-C in 3-D Breast Cancer Models Using Cell Biological and In Silico Approaches

5a. CONTRACT NUMBER

5b. GRANT NUMBER
W81XWH-06-1-0315

5c. PROGRAM ELEMENT NUMBER

6. AUTHOR(S)
Agne Taraseviciute
Peter Lloyd Jones, Ph.D.

Email:

5d. PROJECT NUMBER

5e. TASK NUMBER

5f. WORK UNIT NUMBER

7. PERFORMING ORGANIZATION NAME(S) AND ADDRESS(ES)

University of Pennsylvania
Philadelphia, PA 19104

8. PERFORMING ORGANIZATION REPORT NUMBER

9. SPONSORING / MONITORING AGENCY NAME(S) AND ADDRESS(ES)
U.S. Army Medical Research and Materiel Command
Fort Detrick, Maryland 21702-5012

10. SPONSOR/MONITOR'S ACRONYM(S)

11. SPONSOR/MONITOR'S REPORT NUMBER(S)

12. DISTRIBUTION / AVAILABILITY STATEMENT
Approved for Public Release; Distribution Unlimited

13. SUPPLEMENTARY NOTES
Original contains colored plates: ALL DTIC reproductions will be in black and white.

14. ABSTRACT The extracellular matrix (ECM) glycoprotein tenascin-C (TN-C) has already been implicated in both breast cancer development and progression (Jones, 2001 & Jakhola,1998). TN-C has also been independently linked to poor prognosis in breast cancer (Suwiwat, 2004). However, the mechanisms by which TN-C exerts its effects on human mammary epithelial cells within an appropriate tissue context have not been elucidated. The purpose of this training grant is to determine the mechanism by which TN-C perturbs normal tissue architecture in three-dimensional (3-D) organotypic cultures of human mammary epithelial cells by focusing on cell-cell junctions, adherens junctions in particular, as well as activation of receptor tyrosine kinases, namely EGFR and c-met. Furthermore, as 3-D organotypic cultures are becoming more widely used in the biological community, we sought to develop a computational tool for objective evaluation of three-dimensional (3-D) architecture in organotypic cultures, in order to be able to determine the global effects of TN-C and other ECM components as well as oncogenes on overall tissue architecture. By elucidating the effects of TN-C on tissue architecture and gaining insights into the mechanisms involved, we hope to better understand how to rationally target the ECM, and TN-C in particular, for therapy in premalignant and malignant breast lesions.

15. SUBJECT TERMS
ECM, tenascin-C, mammary tissue architecture, Stroma, Active Contours, 3-D Computational Modeling, c-met

16. SECURITY CLASSIFICATION OF:			17. LIMITATION OF ABSTRACT	18. NUMBER OF PAGES	19a. NAME OF RESPONSIBLE PERSON
a. REPORT	b. ABSTRACT	c. THIS PAGE			USAMRMC
U	U	U	UU	50	19b. TELEPHONE NUMBER *(include area code)*

Table of Contents

Introduction

The extracellular matrix (ECM) glycoprotein tenascin-C (TN-C) has already been implicated in both breast cancer development and progression (Jones, 2001 & Jakhola,1998). TN-C has also been independently linked to poor prognosis in breast cancer (Suwiwat, 2004). However, the mechanisms by which TN-C exerts its effects on human mammary epithelial cells within an appropriate tissue context have not been elucidated. The purpose of this training grant is to determine the mechanism by which TN-C perturbs normal tissue architecture in three-dimensional (3-D) organotypic cultures of human mammary epithelial cells by focusing on cell-cell junctions, adherens junctions in particular, as well as activation of receptor tyrosine kinases, namely EGFR and c-met. Furthermore, as 3-D organotypic cultures are becoming more widely used in the biological community, we sought to develop a computational tool for objective evaluation of three-dimensional (3-D) architecture in organotypic cultures, in order to be able to determine the global effects of TN-C and other ECM components as well as oncogenes on overall tissue architecture. By elucidating the effects of TN-C on tissue architecture and gaining insights into the mechanisms involved, we hope to better understand how to rationally target the ECM, and TN-C in particular, for therapy in premalignant and malignant breast lesions.

Body

In task 1 we proposed to determine whether TN-C disrupts adherens junctions in normal mammary epithelial tissue structures. We initially carried out these experiments on two-dimensional (2-D) tissue culture plastic, where differences in the distribution pattern of b-catenin were noted upon culture in the presence of TN-C. Namely, there was increased accumulation of b-catenin in the nucleus and loss of b-catenin from the cell membrane. Upon closer inspection it became apparent that epithelial cells cultured in the presence of TN-C fail to 'zipper' together, creating gaps between the cells. It is likely that the mechanism for this involves tension forces generated on the actin cytoskeleton and the family of Rho GTPases, which control the dynamics of the actin cytoskeleton. In fact, it has been shown in fibroblasts that TN-C downregulates RhoA, which may be responsible for the lack of traction forces needed to bring cells close together (Midwood, 2002). These studies are currently being investigated in 3-D cultures. Briefly, normal human mammary epithelial cells (MCF-10A) are cultured in a reconstituted basement membrane in the presence or absence of TN-C. Whereas in the absence of TN-C, epithelial cells organize into spherical and smooth acinar structures, a high degree of dysmorphology is apparent when the cells are cultured in the presence of TN-C. As some of the antibodies commonly used in 2-D are not suitable for immunofluorescent analysis in whole 3-D cultures, their expression patterns will have be determined in frozen sections from 3-D cultures. These experiments are ongoing in order to determine whether loss of b-catenin from the cell membrane and accumulation in the nucleus also occurrs in the appropriate 3-D tissue context. To further investigate loss of b-catenin from the cell membrane, we conducted 2-D studies using substrate-bound TN-C to determine levels of associated E-cadherin/b-catenin as well as E-cadherin/a-catenin (another major component of adherens junctions) using immunoprecipitation (IP). We could not detect any differences in the levels of associated E-cadherin/b-catenin and E-cadherin/a-catenin in the presence or absence of TN-C. However, these were our findings in 2-D, and they do not necessarily suggest that the association between the aforementioned proteins will be the same in 3-D cultures. One limitation of 3-D cultures is the amount of protein that can be acquired from cells liberated from the surrounding basement membrane, and since large quantities of protein are required for IPs, it will be necessary to pool protein from 3-D cultures in order to obtain satisfactory quantities of protein for protein interaction analysis. At the moment, we are investigating the absolute minimum of protein required in order to detect E-cadherin/b-catenin and E-cadherin/a-catenin interactions, and at the moment the range of 60-100mg of protein has proven to be sufficient in 2-D cultures.
We are currently continuing to investigate the levels of cytoplasmic versus nuclear b-catenin in 3-D cultures, which will aid us in corroborating the IP studies for E-cadherin/b-catenin interactions. In 2-D cultures we were already able to show differences in the levels of nuclear

and cytoplasmic b-catenin, namely the nuclear to cytoplasmic ratio was higher in cells cultured on substrate-bound TN-C.

In task 2, we proposed to determine whether TN-C alters normal mammary tissue architecture by modulating the activity or distribution of the epidermal growth factor receptor (EGFR). We have conducted preliminary studies in 2-D cultures of normal human mammary epithelial (MCF-10A) cells and demonstrated the activation of the EGFR by Western immunoblotting in response to EGF present in MCF-10A growth medium. Since EGF is already a component of the growth medium, it is likely that the EGFR is always activated. However, it will be of interest to explore whether TN-C increases this activation, or if it indeed maintains EGFR activation even upon withdrawal of EGF from (or bloacked of EGF in) the growth medium. Similarly, in order to explore the possibility that EGFRs are clustered due to integrins, indirect immunofluorescence studies for EGFR and integrins (in frozen sections from 3-D mammary epithelial cultures) are underway and blockade of integrins will be performed in order to establish their involvement in EGFR activation.

In task 3, we proposed to validate the effects of TN-C on mammary tissue architecture via AJ disruption and EGFR activation and/or distribution using a novel 3-D computer modeling approach. The computational modeling of 3-D mammary acini has been further developed in order to provide 3-D renditions of individual acini which can be compared to perfect ellipsoids (individual best-fitting ellipsoids for each acinus). This comparison allowed us to derive an objective measure of the effects of TN-C on tissue architecture by measuring surface roughness, reported as the root mean square (RMS), derived from the difference in the Euclidian distance between the acinus and the ellipsoid. Upon analyzing 103 individual acini, we were able to objectively measure a 1.6-fold increase in surface roughness in 3-D mammary acini cultured in the presence of TN-C. Furthermore, it was also possible to calculate the acinar volume using 3-D acinar renditions, which revealed no difference in the presence or absence of TN-C. This finding, coupled with previous knowledge that proliferation of epithelial cells is increased in the presence of TN-C, while apoptosis is unaffected, suggested that the hyper-proliferating cells were accumulating within the lumens of the acini. We thus hypothesized that TN-C controls c-met, a receptor tyrosine kinase implicated in lumen formation and branching morphogenesis during mammary gland development (Tsarfaty, 1992) which is a proto-oncogene that is commonly upregulated in breast cancer (Lengyel, 2005). TN-C led to a 1.4-fold increase in c-met expression in the epithelium, without upregulating its ligand, HGF. These findings are of interest not only because they identify the regulation of a proto-oncogene by TN-C but also because human breast cancer tissues exhibiting a TN-C-enriched stroma are often in close apposition to malignant epithelium that is highly disorganized and positive for c-met.

Key Research Accomplishments

- TN-C increases epithelial cell proliferation in 3-D mammary epithelial cell cultures
- TN-C does not affect apoptosis in 3-D mammary epithelial cell cultures
- TN-C disrupts normal mammary epithelial tissue architecture
- Active contours-based computational argorithm developed
    - Surface roughness (RMS) measurements obtained for 103 acini
        - These measurements have allowed for objective assessment of 3-D tissue disorganization
        - TN-C increases surface roughness
    - Acinar volume measurements obtained
        - TN-C has no effect on acinar volume
- The computational information shed light on the mechanism for the actions of TN-C
    - The proto-oncogene c-met is implicated in luminal filling
    - TN-C upregulates c-met, but not HGF

Reportable Outcomes

Manuscripts:

1. Agne Taraseviciute, Benjamin Vincent & Peter Lloyd Jones Stromal tenascin-C promotes epithelial cell proliferation to disrupt normal mammary tissue architecture at the luminal level, submitted to Cancer Research, March 2007.

Abstracts:

1. Agne Taraseviciute, Benjamin T. Vincent & Peter L. Jones. Stromal Tenascin-C in Breast Cancer: Effects on Mammary Epithelial Tissue Architecture. Western Student Medical Research Forum (WSMRF), February 2006.
2. Agne Taraseviciute, Benjamin T. Vincent & Peter L. Jones. Disruption of Normal Human Mammary Gland Architecture by Tenascin-C Revealed and Quantified Using an Active Contours-based Computational Model. Institute for Medicine and Engineering Symposium, May 2006.
3. Agne Taraseviciute, Kathryn Horwitz, Troy Stevens, Ilya Levental, Audra Goach-Sostarecz, Paul Janmey and Peter Lloyd Jones. Involvement of Macrovascular Tenascin-C in Breast Cancer Metastasis to the Lung. EMBO, June 2006.
4. Agne Taraseviciute, Kathryn Horwitz, Troy Stevens, Ilya Levental, Audra Goach-Sostarecz, Paul Janmey and Peter Lloyd Jones. Involvement of Tenascin-C in Mediating Breast Cancer Metastasis to the Lung: Effects on Endothelial Cell Surface Stiffness. ASCB, December 2006.

Presentations:

1. Agne Taraseviciute, Benjamin T. Vincent & Peter L. Jones. Stromal Tenascin-C in Breast Cancer: Effects on Mammary Epithelial Tissue Architecture. Western Student Medical Research Forum (WSMRF), February 2006.

Conclusion

We have demonstrated that stromal TN-C disrupts normal mammary tissue architecture in 3-D organotypic cultures by increasing proliferation and upregulation of c-met leading to filled lumens within the acini. Furthermore, we have developed a computational tool which measures surface roughness of mammary acini in order to quantify 3-D acinar architecture. This allowed us to objectively measure the effects of TN-C in otherwise quite heterogeneous cultures. The computational tool was furthermore used to measure acinar volume, which remained regardless of the presence of TN-C. Since proliferation was increased, and apoptosis and volume were unchanged in the cultures exposed to TN-C, it led us to hypothesize and subsequently show that luminal filling was occurring in TN-C-exposed cultures, and that this process involves the receptor tyrosine kinase c-met. Thus, it was the findings obtained through computational biology that were informative for and paved the way for cell biology. By understanding how TN-C perturbs mammary tissue architecture, we can begin to envision using a therapeutic approach to target the ECM and block the pathways involved in breast cancer pathogenesis.

References

Jones PL. Extracellular matrix and tenascin-C in pathogenesis of breast cancer. Lancet 2001;357(9273):1992-4.

Jahkola T, Toivonen T, Nordling S, von Smitten K, Virtanen I. Expression of tenascin-C in intraductal carcinoma of human breast: relationship to invasion. Eur J Cancer 1998;34(11):1687-92.

Lengyel E, Prechtel D, Resau JH, et al. C-Met overexpression in node-positive breast cancer identifies patients with poor clinical outcome independent of Her2/neu. Int J Cancer 2005;113(4):678-82.

Midwood KS, Schwarzbauer JE. Tenascin-C modulates matrix contraction via focal adhesion kinase- and Rho-mediated signaling pathways. Mol Biol Cell 2002;13(10):3601-13.

Suwiwat S, Ricciardelli C, Tammi R, et al. Expression of extracellular matrix components versican, chondroitin sulfate, tenascin, and hyaluronan, and their association with disease outcome in node-negative breast cancer. Clin Cancer Res 2004;10(7):2491-8.

Tsarfaty I, Resau JH, Rulong S, Keydar I, Faletto DL, Vande Woude GF. The met proto-oncogene receptor and lumen formation. Science 1992;257(5074):1258-61.

Appendices

Please find enclosed below a reprint of our manuscript submitted to Cancer Research entitled “Stromal tenascin-C promotes epithelial cell proliferation to disrupt normal mammary tissue architecture at the luminal level”.

Stromal tenascin-C promotes epithelial cell proliferation to disrupt normal mammary tissue architecture at the luminal level

Agne Taraseviciute[1,2*], Benjamin Vincent[3] & Peter Lloyd Jones[2†]

Department of Cell & Developmental Biology[1], University of Colorado at Denver & Health Sciences Center, Aurora, CO; Institute for Medicine & Engineering, Department of Pathology & Laboratory Medicine[2], University of Pennsylvania, PA; Department of Experimental Psychology[3], University of Bristol, United Kingdom

** Both authors contributed equally to this work*

†Address for correspondence:
Peter Lloyd Jones, Ph.D.
Department of Pathology & Laboratory Medicine
Institute for Medicine & Engineering
1010 Vagelos Research Laboratories
University of Pennsylvania
Philadelphia, PA 19104-6383

Voice: (215) 898 0048
Fax: (215) 573 6815
e-mail: jonespl@mail.med.upenn.edu & ben.vincent@bristol.ac.uk

Abstract

Induction of tenascin-C (TN-C), a stromally-derived extracellular matrix (ECM) glycoprotein, is associated with breast cancer development and progression, yet its role in this disease remains obscure. To investigate the effects of TN-C on normal human mammary epithelium, MCF-10A cells were cultivated in a three-dimensional (3-D) reconstituted basement membrane, either with or without exogenous TN-C. Whereas control cells formed polarized acinar structures, complete with a continuous basement membrane and a central lumen (resulting from site-specific apoptosis), exposure to TN-C provoked selective loss of basement membrane and increased epithelial cell proliferation, without affecting apoptosis. To determine how these changes alter mammary epithelial tissue structure and function, an imaging algorithm was developed to generate 3-D renditions of mammary acini, which were then used to assess and quantify acinar topography and volume. Although TN-C increased acinar surface roughness, it had no effect on volume. Based on these results, we hypothesized that TN-C promotes epithelial cell proliferation within lumens, and that this process might involve c-met, a receptor tyrosine kinase which is over-expressed in breast tumors, where it is believed to affect both lumen formation and cell proliferation. Indeed, TN-C-treated acini contained filled lumens and they expressed higher levels of c-met than controls. Importantly, human breast cancers enveloped by a TN-C-rich stroma expressed high levels of epithelial c-met when compared to normal tissue. Collectively, these 3-D studies indicate that TN-C compromises mammary epithelial tissue homeostasis via its effects on basement membrane integrity, c-met expression and luminal epithelial cell proliferation.

Introduction

Breast cancer is the leading cause of cancer deaths in women (1), and although mortality rates have declined over the past few decades (2), this disease still accounts for more than 40,000 annual deaths in the United States alone (3). Until recently, most pre-clinical and clinical studies focused on the transformed epithelium as a key component in the diagnosis and treatment of breast cancer (4). Compelling evidence, however, demonstrates that the adjacent stromal microenvironment, which includes the extracellular matrix (ECM), represents a critical determinant of normal breast development (5-7), and it plays a major role in breast tumor initiation, progression and metastasis (8-11). Seminal studies by Bissell and colleagues have elegantly established the importance of the ECM microenvironment in regulating normal and aberrant mammary tissue organization and function (12). For example, when cultured in a compliant, laminin-enriched ECM, normal breast epithelial cells produce an endogenous basement membrane, which drives the formation of polarized, spherical acinar structures with central, hollow lumens. When provided with lactogenic hormones, these acini can mimic the mammary gland *in vivo* at the functional level, exemplified by vectorial secretion of milk proteins into the central lumens (13). Subsequenly, these types of sophisticated 3-D organotypic cultures allowed investigators to study the effects of specific oncogenes, already implicated in breast cancer, on epithelial tissue structure and behavior in a manner that was not possible using conventional 2-D monolayer cultures. For example, over-expression of ErbB2 (a receptor tyrosine kinase mutated or amplified in 25-30% of breast cancers (14) in normal mammary epithelial cells cultured

in 3-D results in a multi-acinar, hyper-proliferative phenotype i.e. ErbB2 promotes luminal filling (15). Similarly, co-expression of cyclin D1 and the anti-apoptotic protein Bcl-2 generates a “filled lumen” phenotype (16). In contrast, mammary epithelial cells transformed with either cyclin D1 or with the human papilloma virus (HPV)-16 E7 oncogene alone form individual acini which contain a lumen, but are generally of increased size (16). Thus, different oncogenes exert site-specific effects on 3-D mammary acinar architecture. Since tissue architecture in itself has been shown to control the functions of these genes, i.e. phenotype can dominate over genotype (17), understanding the generation and loss of form in the breast is now recognized as a key step in breast cancer research and therapy (18).

The fact that stromal-epithelial interactions are critical for tumorigenesis is exemplified by experiments showing that blocking interactions between breast cancer cells and their surrounding ECM microenvironment can lead to reversion of the malignant epithelial phenotype *in vivo* (19). Consistent with these studies, alterations in the stromal compartment have been shown to contribute to breast cancer development and progression. For example, ectopic induction of the ECM-degrading protease, stromelysin-1 (MMP-3), in the mouse mammary gland leads to inappropriate destruction of the basement membrane, and subsequent transformation of the adjacent epithelium (20). This process is accompanied by induction of stromal TN-C (21), loss of E-cadherin from cell-cell junctions (22), and activation of the small GTPase, Rac1b, which aids in the generation of DNA-damaging reactive oxygen species (23). Recent work has also demonstrated that changes in the mechanical properties of the breast stromal ECM dictate whether epithelial cells will behave in either a normal or malignant fashion (24).

For example, when normal breast epithelial cells are maintained in a stiffer ECM microenvironment compared to normal, proliferation increases, adherens junctions are destabilized, and lumen formation is inhibited, resulting in loss of normal tissue organization (24). Collectively, these and other studies demonstrate that both the chemical and physical nature of the stromal ECM are critical determinants of breast development, homeostasis and disease. Thus, identifying the function(s) of specific ECM components that are expressed in the breast tumor stroma represents a key step in understanding this disease.

Tenascin-C is a large ECM glycoprotein that is generally absent in the normal, resting, adult breast (25), yet its expression increases in the stroma of the involuting mouse mammary gland (26), as well as in the stroma surrounding experimental and human breast carcinomas (27-29). Furthermore, levels of stromal TN-C expression have been reported to correlate with breast tumor grade and stage (28, 30). Of note, in studies investigating the role of various ECM proteins in breast cancer, TN-C was the only ECM component found to serve as a negative predictor of overall patient survival (28, 30). In addition, TN-C was recently shown to be 1 of 54 genes involved in mediating breast cancer metastasis to the lung, and it represents 1 of 18 genes used for breast cancer patient prognostication leading to pulmonary metastasis (31). Despite these studies implicating TN-C in breast tumorigenesis and metastasis, its effects on human mammary epithelial tissue architecture have not been evaluated objectively in an appropriate 3-D tissue context. This is of importance, since mammary epithelial cells exhibit radically different forms of behavior in 2-D versus 3-D cultures (5, 18, 26, 32, 33). To redress this, we quantified how stromal TN-C affects normal human mammary

epithelial 3-D tissue structure with the aim that this would provide new clues regarding its function in breast cancer. Herein, we describe the development of a novel imaging tool which allowed us to discover that TN-C not only promotes expression of c-met, a proto-oncogene associated with a poor prognosis in breast cancer, but that this event is accompanied by loss of normal mammary epithelial tissue architecture, characterized by disruption of the basement membrane, and increased cell proliferation leading to inappropriate filling of the central lumen.

Materials & Methods

Reagents

Cell culture medium (DMEM, F12/Ham's)), horse serum, 0.25% trypsin-EDTA and penicillin/streptomycin were from Invitrogen (Carlsbad, CA**).** Epidermal growth factor (EGF) was purchased from Peprotech (Rocky Hill, NJ). Cholera toxin, hydrocortisone, insulin and normal goat serum (NGS) were from Sigma-Aldrich (St. Louis, MO). Phenol Red-free, growth factor-reduced Matrigel was from BD Biosciences (San Jose, CA). Human TN-C protein was from Chemicon (Temecula, CA). Mouse-anti-human TN-C antibody was from Novocastra (Newcastle-upon-Tyne, UK). Laminin V (human-specific) and α6 integrin antibodies were from Chemicon, while Ki-67 and cleaved caspase-3 antibodies were from Zymed (Invitrogen; Carlsbad, CA) and Cell Signaling (Danvers, MA), respectively. c-met antibody was from R&D Systems (Minneapolis, MN). Goat anti-mouse $F(ab')_2$ fragments were from Jackson ImmunoResearch (West Grove, PA). Donkey anti goat-HRP secondary antibody was from Santa Cruz Biotechnology (Santa Cruz, CA). All Alexa Fluor-conjugated (Alexa Fluor 488 and 594) secondary antibodies were from Molecular Probes (Invitrogen; Carlsbad, CA). 16% paraformaldehyde was from Electron Microscopy Sciences (Hatfield, PA). The Vectastain ABC and DAB kits, species-specific biotinylated secondary antibodies, and Vectashield mounting medium containing DAPI were from Vector Laboratories (Burlingame, CA). Cytoseal and Clear-Rite 3 were from Richard-Allan Scientific (Kalamazoo, MI). Pre-cast 4-20% precise protein gels were from Pierce (Rockford, IL).

Immunohistochemistry (see supplement)

Human breast tissue microarrays were from Cybrdi (Frederick, MD) and US Biomax (Rockville, MD). Pathological evaluation of tissue sections was validated by an experienced pathologist. A pronase-based antigen retrieval process was used for TN-C immunohistochemistry, while citrate buffer was used for double immunostaining for TN-C and c-met. Incubation with TN-C or c-met antibody (1:50) was performed overnight at 4°C. Slides were washed in 1% PBSA (1% BSA in PBS) followed by 0.1% PBSA, and incubated with biotinylated anti-mouse IgG (for TN-C), and biotinylated anti-goat IgG (for c-met). After washing, slides were incubated with the streptavidin/peroxidase ABComplex for 30 minutes at RT. Sections were then incubated for 5 minutes with DAB (for TN-C) or VectorNovaRED (for c-met) substrates at RT. Sections were counter-stained with hematoxylin QS (for TN-C alone), rinsed, dehydrated, cleared in CitriSolv, and mounted. For sections in which double-immunolabeling was performed, after washing, sections were blocked. Incubation with TN-C antibody (1:50) was subsequently performed. Slides were washed, and incubated with biotinylated anti-mouse IgG for 45 minutes at RT. After washing, slides were incubated with the streptavidin/alkaline phosphatase (AP) ABComplex for 30 minutes at RT. Sections were then incubated with Vector Blue AP substrate. Sections co-immunostained for c-met and TN-C were mounted using Vectamount AQ. Images were captured using a Nikon 90i microscope equipped with a Nikon DXM1200 digital camera at 20X magnification (NA 0.75).

Cell Culture (see supplement)

The MCF-10A human mammary epithelial cell line was obtained from the American

Tissue Culture Collection ((ATCC), Manassas, VA). Cells were cultured in a 3-D ECM (Matrigel) using an overlay method, originally developed by Bissell and colleagues (34, 35). Cells were plated on a solidified layer of Matrigel either with or without 10μg/ml purified human TN-C protein, and the 3-D cultures were maintained at 37°C in a humidified incubator with 5% CO_2. The overlay assay medium was changed every 4 days and cultures were maintained for 4-8 days.

Immunocytochemistry

3-D cultures were fixed, washed and stained according to standard methods using primary antibodies diluted in blocking solution (laminin V, 1:100; α6 integrin, 1:200; Ki-67, 1:50; cleaved caspase-3, 1:100; c-met, 1:50) for 12 h at RT. This was followed by incubation in Alexa Fluor-conjugated species-specific secondary antibodies diluted in IF buffer containing 10% NGS (either Alexa Fluor 488 or 594 conjugated antibodies, 1:100). Z-stacks of images at 1 or 2 μm intervals using a laser scanning confocal microscope (Zeiss LSM 510, oil-immersion 25X objective, NA 0.8).

Nuclear Counts & Computational Biology: (see supplement)

Results

TN-C promotes proliferation & disrupts mammary epithelial tissue organization

Induction of stromal TN-C expression is associated with a wide variety of solid tumors, including those originating in the breast (36). Consistent with this, immunohistochemical analysis of breast tissue microarrays showed that TN-C was absent from normal breast tissue (Figure 1A), but was frequently expressed at high levels in the stroma of malignant and pre-malignant breast lesions, including ductal carcinoma *in situ* (DCIS), where it appeared as a fibrotic band beneath hyperplastic ductal epithelial cells (Figure 1A). Of note, induction of stromal TN-C in DCIS and malignant breast lesions corresponded with loss of normal tissue organization in the adjacent epithelium, which included luminal filling (Figure 1A).

To determine whether TN-C directly affects the structure and function of the normal human mammary epithelium, MCF-10A cells (which do not express TN-C, data not shown), were cultivated for 4 to 8 days in the presence of a reconstituted basement membrane (i.e. Matrigel), either with or without purified, exogenous human TN-C protein. Although control and TN-C-treated cultures both formed 3-D acini, their appearance differed: whereas control acini appeared mostly smooth and spherical (Figure 1B, upper left panel), those exposed to TN-C deviated from this normal structure, exhibiting a more disorganized phenotype (Figure 1B, lower right panel). To begin to delineate these differences in more detail, we first evaluated whether TN-C affects endogenous basement organization (via laminin V immunostaining). Control acini were surrounded by a smooth and continuous basement membrane, which was

disrupted upon exposure to TN-C, resulting in a discontinuous structure exhibiting numerous gaps and folds (Figure 1B, middle & right panels). In addition, epithelial cells appeared to be transiting through gaps in the basement membrane into the surrounding TN-C-enriched microenvironment (Figure 1B, middle & right panels). Since TN-C has already been shown to support cell proliferation and survival in remodeling tissues (37, 38), one possible explanation to account for its ability to alter normal 3-D mammary epithelial tissue architecture is by increasing cell proliferation on the one hand, whilst decreasing luminal apoptosis on the other. Indeed, immunostaining for Ki-67 revealed a significant 1.6-fold increase in epithelial cell proliferation in response to TN-C (Figure 1B, middle panels & Figure 1C; 16.5 +/-2.3 versus 10.6 +/- 1.3; $p<0.009$). Levels of apoptosis within the acinar interior, however, were identical in control and TN-C-treated cultures, as determined by immunostaining for cleaved caspase-3 (Figure 1B, right panels & Figure 1C).

Creating 3-D renditions of mammary epithelial acini

Given that TN-C promoted net increases in mammary epithelial cell proliferation, it is possible that this would compromise 3-D mammary epithelial architecture by increasing acinar volume. Alternatively, increased proliferation may result in accumulation of epithelial cells within the lumen of acini, without affecting volume. Objectively testing these ideas is critical, since different cancer-associated genes have been shown to exert different effects at different locations within 3-D mammary acini (15, 16, 39), and architecture in itself can control breast cancer behavior through modulation of these genes (40). While 3-D ECM-based cultures represent a state-of-the-art method for

examining the behavior of cells in an appropriate *in vivo*-like context, they still remain difficult to analyze, due to the inherent heterogeneity that occurs within these cultures in particular (Figure 1B, left panels), and within biological systems in general (41). To redress this, we developed a quantitative image analysis tool designed to measure the surface roughness and volume of mammary acini in 3-D. Surface roughness was chosen as a parameter, because it is accepted that loss of normal structure not only reflects the state of tumorigenesis, but that loss of normal structure in and of itself may contribute to tumor initiation and progression (42).

To quantify the effects of TN-C on mammary epithelial tissue structure, an active contours-based algorithm was devised to trace the edges of individual mammary acini, delineated by immunostaining for laminin V or a6 integrin, a receptor for laminin V. 2-D images acquired from confocal Z-sections of 1-2 mm sections were used for this procedure (Figure 2A). The green channel from the confocal images formed an 8-bit grayscale image, and after noise removal the blurred image gradients (*dx* and *dy*) were obtained (Figure 2B, upper panels). The active contour for the equatorial z-section was initiated by manually selecting a number of points close to the edge of the acinus (Figure 2B, lower left panel), which were then automatically finalized to create the outline of the edge (Figure 2B, lower right panel). This initial equatorial contour was used to automatically trace the remaining images in the Z-stack for each acinus, resulting in a montage of images (Figure 2C), which were used to check for any errors in tracing. Each montage was used to construct a 3-D rendition of each acinus (Figure 2D), which was then evaluated for surface roughness by comparing the 3-D rendition to

a customized, best-fitting ellipsoid, which represents a 'perfectly smooth' surface (Figure 3A).

TN-C increases acinar surface roughness, but has no effect on volume

Having developed the means to generate 3-D renditions of acini, we objectively examined the effects of TN-C on tissue architecture in 103 individual acini generated via more than 3 independent experiments. Even prior to calculating surface roughness, 3-D reconstructions of individual acini revealed that TN-C had a profound effect on normal mammary epithelial tissue architecture (Figure 3A). Specifically, when compared to control cultures, numerous protrusions and indentations were apparent in acini cultured in the presence of TN-C (Figure 3A). Analysis of differences in protrusions and indentations in each Z-stack of the acinus confirmed that TN-C promotes a greater degree of deviation from the perfect ellipsoid compared to control (Figure 3B). Next, we calculated surface roughness in control and TN-C-treated acini by calculating a root-mean-square (RMS) value based on the differences between Euclidian distances of 3-D acinar renditions versus a best-fitting ellipsoid (Figure 3B). Smooth acini generated lower RMS values when compared to more disorganized acini, which produced higher RMS values. Of note, TN-C-treated cultures exhibited a 1.7-fold increase in mean RMS value (RMS = 4.96±0.38), when compared to control cultures (RMS = 2.98±0.18, $p<0.001$) (Figure 3C). As well as quantifying acinar surface roughness, active contours-generated 3-D acinar renditions allowed us to make additional structural measurements. By simply 'unwrapping' 3-D renditions, Mercator projections were produced, allowing for

visualization of the finer surface features in control and TN-C-treated acini, in a topographical “map” format (Figure 3-D).

The distribution of RMS values and acinar volumes for both control and TN-C-treated conditions were also analyzed. Using logistic regression analysis, we calculated performance in terms of percent correct classification of condition with a mean ± standard deviation, obtained using a bootstrap technique (43). Using RMS measurements alone resulted in good discrimination performance of 69.8% ± 4.8 (Figure 4E, left graph). In contrast, taking volume measurements alone into account resulted in a low performance of 56.6% ± 4.7 (Figure 4E, right graph). However, a multiple logistic regression taking both RMS and volume into account yielded a higher performance of 79.5% ± 4.4, i.e. the control and TN-C-exposed acini could be segregated with approximately 80% accuracy (Figure 3F). Thus, although TN-C has very little effect on acinar volume compared to surface topography, upon consideration of both volume and surface roughness (reflected by RMS values) it becomes possible to make inferences regarding the culture conditions of individual acini, i.e. whether they were cultured in the absence or presence of TN-C.

TN-C promotes luminal filling & increases c-met expression

When coupled with immunofluorescence data for laminin V, Ki-67 and cleaved caspase-3, the active contours-derived measurements indicated that TN-C not only compromises basement membrane integrity, resulting in increased surface roughness, but that TN-C also increases epithelial cell proliferation and subsequent accumulation of these cells within the lumen of acini, given that the mean acinar volume was the same in control

and TN-C-treated cultures. In keeping with this latter idea, closer inspection of DAPI-stained nuclei at multiple levels within Z-stacks confirmed that control acini possess a centrally-located, cell-free lumen, lined by a single layer of epithelial cells (Figure 4A, upper left panel). In contrast, acini formed in the presence of TN-C contain multiple, discrete lumens that are lined by multiple epithelial cell layers (Figure 4A, upper right panel).

Based upon these findings, we chose to explore the relationship between TN-C and c-met (i.e. the hepatocyte growth factor (HGF) receptor). C-met is a proto-oncogene which is over-expressed in breast cancer (44), and it controls both tumor cell proliferation and lumen formation in the mammary gland (45). As well, increases in expression of TN-C in the tumor stroma and c-met in the adjacent transformed epithelium have both been independently linked to poor outcome in breast cancer patients (36, 46-48), and elevated expression of c-met in breast tumors represents a more reliable marker of poor prognosis in a sub-set of breast tumors when compared to tumor size (44). Given these facts, we hypothesized that TN-C promotes epithelial cell proliferation and luminal filling by inducing c-met. Consistent with this, immunofluorescence staining indicated that c-met levels were increased in TN-C-treated cultures when compared to controls (Figure 4A, lower panels). Western immunoblotting supported these findings, revealing that TN-C significantly upregulates c-met expression by more than 1.4-fold, when normalized to β-actin, in 3-D cultures of human mammary epithelial cells cultured for 4 days (Figure 4B & 4C). Please note that c-met is expressed as a 170 kDa pro-form, and a 140 kDa processed form, hence the appearance of 2 bands in western immunoblots (Figure 4B). In parallel, we assessed

the levels of HGF in conditioned media derived from cultures, and found that TN-C had no effect on the levels of secreted HGF (Figure 4B).

Breast tumors expressing stromal TN-C exhibit high levels of epithelial c-met

Finally, to begin to determine the relevance of our 3-D modeling studies to the pathogenesis of human breast cancer *in vivo*, we co-immunostained normal and breast cancer tissue microarrays for TN-C and c-met. Double immunohistochemistry demonstrated that in contrast to normal breast tissue (Figure 5, upper panels), breast tumors expressing high levels of stromal TN-C also expressed high levels of c-met in the adjacent epithelium (Figure 5, lower panels). Thus, induction of stromal TN-C corresponds with elevated levels of epithelial c-met in human breast cancers.

Discussion

It is now fully accepted that the tissue microenvironment, which includes the ECM, controls breast development, differentiation, homeostasis, as well as cancer initiation and progression (8, 40, 49-51). In further support of this, we and others have shown that stromal TN-C expression accompanies breast cancer initiation and progression (27, 36, 38, 48). The underlying mechanisms for the actions of TN-C on the human mammary epithelium, however, were lacking. In this study, we demonstrated that TN-C disrupts normal tissue architecture by compromising the integrity of the basement membrane and promoting a net increase in cell proliferation. Using a novel image-processing and analysis tool, we objectively evaluated changes in 3-D acinar structure in response to TN-C. Although TN-C increased epithelial cell proliferation, upon measuring the volume of mammary acini, we discovered that this parameter was not affected by TN-C. This finding allowed us to hypothesize, and thereafter show, that TN-C promotes luminal filling, which may potentially occur via upregulation of c-met. Therefore, by applying a quantitative approach to analyze 3-D mammary epithelial tissue structures, we were able to link the presence of stromal TN-C to pathological changes that are relevant to human breast tumorigenesis *in vivo,* including disruption of normal basement membrane organization, induction of c-met, increased cell proliferation and filling of the central lumen (Figure 6).

Previous studies involving transformed 2-D monolayers of mammary epithelial cells demonstrated that TN-C promotes cell proliferation (52), as well as epithelial-mesenchymal transformation (EMT) in breast and colorectal cancer cell lines (53, 54). TN-C also supports cell migration in gliomas and colorectal adenocarcinomas (55), as

well as tumor angiogenesis in melanomas (56). Mechanistically, it has been postulated that TN-C controls one or more of these processes in the mammary epithelium and other tissues via its ability to impact genome stability (38), cell cycle progression (57), production of MMPs (58), expression of VEGF (56), as well as activation of receptor tyrosine kinases, including epidermal growth factor receptors (36, 59). In this study, we have added c-met to the expanding list of molecules that TN-C regulates in breast cancer. Collectively, these and other studies indicate that TN-C represents a reliable diagnostic marker of malignancy, and it may also represent a suitable target for breast cancer treatment (48). Consistent with this, TN-C radioimmuno-, RNAi- and aptamer-based strategies are already being evaluated for tumor targeting, stabilization of malignant glioma and treatment of non-Hodgkin's lymphoma (60-65).

In 3-D mammary epithelial cultures treated with TN-C we noted deficits in the production, assembly and/or stability of the endogenous basement membrane, as well as cellular trans-migration through this structure into the surrounding ECM. It is plausible that TN-C induces this phenotype by inducing matrix metalloproteinases (MMPs), an effect that has already been described for synovial fibroblasts, which produce MMP-9 when interacting with mixed substrates of TN-C and fibronectin (58). However, gelatin substrate zymography did not reveal differences in MMP-2 or MMP-9 levels or activity in response to TN-C (data not shown). Nonetheless, TN-C may stimulate MMPs that are not detectable via gelatin zymography, including MMP-12, which is upregulated by TN-C in 3-D cultures of gliomas (66), and MMP-3, which is activated in the involuting breast together with TN-C (67). It is also possible that TN-C disrupts mammary epithelial tissue architecture in an MMP-independent manner

through activation of other ECM-degrading enzymes, such as the serine proteinase, uPA, another reliable prognostic marker in breast cancer (68), and one that is expressed in the tumor stroma together with TN-C (69). Alternatively, TN-C may disrupt the basement membrane in a protease-independent manner. For example, recent studies have shown that invasion and metastasis by oral squamous cell carcinomas is associated with co-deposition of laminin V and TN-C, and that these molecules form a physical complex (70). Thus, TN-C may compromise normal deposition and assembly of the laminin V-enriched (and perhaps degraded) basement membrane in tumors. This finding is also of interest because clinical and experimental studies of muscular dystrophy show that disappearance of the basement membrane corresponds with the induction of TN-C (71, 72). Since loss of the laminin receptor dystroglycan in mammary epithelial cells also leads to disruption of polarity and functional differentiation in 3-D cultures (73), induction of stromal TN-C may perturb basement membrane-dependent mammary epithelial differentiation and homeostasis by inhibiting dystroglycan incorporation and/or function. In support of the idea that TN-C is incompatible with the presence of an intact basement membrane, we have already shown that in the involuting mouse mammary gland, the appearance of TN-C coincides with loss of a functional basement membrane (26). Furthermore, addition of TN-C to mouse mammary epithelial cell cultures that differentiate in response to exogenous BM inhibits this process, whereas addition of basement membrane to TN-C-producing murine mammary gland myoepithelial cells inhibits TN-C mRNA production (26). As well, ectopic activation of MMP-3 in the lactating mammary gland results in premature involution, and this is accompanied by induction of stromal

TN-C (21). Future studies will aim to define the reciprocal functions and interactions between the basement membrane and TN-C in the normal and transformed breast.

Another major finding of this study is that TN-C promotes luminal filling of mammary ductal structures, a hallmark of specific types of pre-invasive and invasive breast lesions, including cribriform DCIS and infiltrating ductal carcinomas (12), both of which are surrounded by high levels of stromal TN-C (Taraseviciute & Jones, unpublished data). Luminal filling may occur when increases in cell proliferation are coupled with deficits in central apoptosis within the acinar interior. For example, luminal filling has been noted when cyclin D1 is over expressed with the anti-apoptotic protein Bcl-2 (39). In our studies, however, central apoptosis was not inhibited, suggesting that TN-C controls an alternative pathway leading to luminal filling. Accordingly, we focused on c-met, a proto-oncogene that is not only required for normal breast development (74), but also for increased cell proliferation and invasion through the ECM (75). Furthermore, and in common with TN-C, overexpression of c-met has been linked with poor prognosis and a high risk of metastasis (76, 77). At a histological level, c-met over expression occurs in invasive ductal breast tumors bearing aberrant lumens (44), and activation of c-met by its ligand HGF has been shown to stimulate extensive development of branched structures by mammary epithelial cells cultured in 3-D (78). Thus, it is plausible that TN-C-dependent induction of c-met contributes to increased surface roughness by promoting a branched-like phenotype, that manifests itself in our system as increased surface roughness. In support of this, TN-C is expressed around the neck of the breast bud and portions of the ducts during development (79), and we have shown that stromal TN-C also promotes epithelial branching morphogenesis in the

developing lung (80) and in pulmonary capillary networks (81).

Although we have not yet determined how TN-C and c-met converge to regulate mammary epithelial tissue behavior, (i.e. we have not yet determined the activation state of c-met in TN-C-treated cultures), it is recognized that c-met collaborates with c-myc to promote breast tumorigenesis (77). This finding is of interest because TN-C induces c-myc expression in 3-D cultures of mouse mammary epithelial cells (5). Future studies will be aimed at determining how TN-C regulates c-met expression, and whether it also controls other pathways that collaborate with this receptor. To this end, we have recently discovered that activated c-met forms a complex with activated EGFRs in MCF-10A cells (Taraseviciute & Jones, unpublished). Since we have already shown that TN-C potentiates the activity of EGFRs (82), and EGFRs cross-modulate c-met activity (83), it is plausible that TN-C not only upregulates c-met expression, but that it indirectly controls its activity via interactions with EGFRs.

In summary, our combined use of organotypic and computational 3-D modeling approaches allowed us to discern that TN-C compromises mammary epithelial tissue homeostasis via its effects on basement membrane integrity, c-met expression and epithelial cell proliferation at the luminal level. Above all, these studies reinforce the idea that microenvironmental cues originating with the tumor stroma function in a dominant and paracrine fashion to control the expression and function of genes already associated with the development and progression of breast cancer.

Figure 1 Effects of TN-C on normal 3-D mammary epithelial tissue architecture **(A)** Representative photomicrographs showing tissue sections from the normal human mammary gland (top panel) and ductal carcinoma *in situ* (DCIS; lower panel). TN-C is not expressed in the normal tissue, but it appears as a narrow (brown) band surrounding the hyper-proliferating ducts in DCIS. *Scale bar, 50μm*. **(B)** Representative phase contrast photomicrographs showing the morphology of MCF-10A acini cultured in Matrigel, using an overlay assay, either with or without TN-C for 8 days (left panels). Representative photomicrographs showing immunofluorescence staining for laminin V (in green), Ki-67 (in red) and cleaved caspase 3 (in red) in MCF-10A acini cultured in Matrigel, either with or without TN-C for 8 days (middle and right panels). *Scale bars, 50μm*. **(C)** Quantification of Ki-67 immunoreactivity in MCF-10A acini revealed a significant 1.6-fold increase in proliferation in response to TN-C (left panel; n=66 acini; *$p<0.009$). Quantification of cleaved caspase 3 immunoreactivity revealed no difference in the levels of apoptosis in response to TN-C (right panel; n=40 acini; $p=0.68$); *Columns, mean; bars, SEM*.

Figure 2 Computational procedure used to assess mammary epithelial tissue architecture **(A)** A schema delineating the computational procedure used to measure acinar surface roughness and volume. **(B)** The equatorial, i.e. central, 2-D slice from confocal Z-stack images of laminin V immunofluorescence staining (in this example, the 2-D slice is derived from a TN-C-treated 8 day 3-D acinus) was subjected to *dx* and *dy* pre-processing based on immunostaining intensity gradients (top panels). These gradients were then used to manually initiate active contours by selecting multiple

points close to the edge of the acinus, delineated by laminin V immunoreactivity (lower panel, left). After active contour fitting, a final trace of the edge of the central acinar slice was obtained (lower panel, right). **(C)** The trace obtained in (B) was extrapolated to all the subsequent 2-D slices of the laminin V-stained acinus resulting in a montage of traces for each acinus. **(D)** Montages described in (C) were used to render a 3-D projection for each acinus.

Figure 3 TN-C increases surface roughness, but has no effect on 3-D acinar volume **(A)** Examples of 3-D renditions of individual acini (black dotted lines), cultured in the absence (top panel) or presence (lower panel) of TN-C for 8 days. A customized ellipsoid (in red-yellow) was designed and fitted to each individual acinus. **(B)** Change in radius for each acinar slice (black dotted lines) denotes distance away from the perfect ellipsoid for the acini depicted in (A); the red horizontal line at '0' represents the perfect ellipsoid, in the absence of TN-C (top), each slice does not deviate more than a few microns from the perfect ellipsoid, while in the presence of TN-C (lower), these deviations approach 10 microns and more. **(C)** Quantification of 3-D acinar structure was made by measuring the root mean square (RMS; absolute difference from perfect ellipsoid) values for acini cultured for 8 days in 3-D in the absence or presence of TN-C. TN-C evoked a significant 1.8-fold increase in surface roughness ($p=0.024$). **(D)** Topographical representations of 3-D acini displayed as 2-D Mercator projections; protrusions are displayed as yellow and red areas while indentations appear aquamarine and dark blue; the TN-C-treated acinus (lower panel) has larger protrusions and indentations, whereas a control acinus (top panel) represents a much flatter surface

architecture. **(E)** Distribution of RMS values (left panel) and volumes (right panel) for acini cultured in the absence (dotted lines) or presence (solid lines) of TN-C (8 day cultures). **(F)** When surface roughness and volume were both taken into account, acini cultured in the absence (open circles) or presence (filled circles) of TN-C become separable into 2 distinct groups, with the line showing the best linear classification using logistic regression, at a performance of 79.5% (see Results).

Figure 4 TN-C promotes luminal filling and upregulates c-met **(A)** Representative immunofluorescence photomicrographs for laminin V and cleaved caspase-3 (upper panels) confirmed increased luminal filling (lumens are outlined in white dotted lines) of acini cultured in the presence (upper right) versus absence (upper left) of TN-C. Representative immunofluorescence photomicrographs for c-met show increased intensity of c-met staining in the presence of TN-C (lower right) compared to control (lower left). *Scale bars, upper panels - 50μm, lower panels - 25 μm.* **(B)** Representative Western immunoblot analysis reveals that in 4 day MCF-10A cultures, c-met levels are increased in the presence of TN-C while HGF levels remain unchanged. β-actin serves as a loading control. **(C)** Densitometric analysis of c-met levels relative to β-actin reveals a 1.4-fold increase in the presence of TN-C.

Figure 5 H & E and co-immunohistochemistry for c-met and TN-C in normal and breast cancer tissue Representative photomicrographs showing tissue sections from the normal human mammary gland (upper panels) and grade 2 infiltrating ductal carcinoma (lower panels). C-met (red) is expressed at very low levels in the epithelium

and TN-C (blue) is absent from the stroma in the normal tissue (upper right panel), however, both c-met and TN-C are expressed at high levels in infiltrating ductal carcinoma in the epithelium and stroma, respectively (lower right panel). *Scale bar, 50μm*.

Figure 6 Hypothetical schema summarizing how TN-C may alter normal mammary epithelial tissue architecture In the normal mammary gland, epithelial cells are polarized around a hollow lumen, and rest upon a continuous basement membrane. Upon induction of TN-C in the stromal compartment, the basement membrane is disrupted, polarity is lost, and the c-met proto-oncogene is upregulated. C-met interacts with its ligand, HGF, leading to proliferation of the epithelial cells and luminal filling.

Literature Cited

1. Parkin DM, Bray F, Ferlay J, Pisani P. Global cancer statistics, 2002. CA Cancer J Clin 2005;55(2):74-108.

2. Veronesi U, Boyle P, Goldhirsch A, Orecchia R, Viale G. Breast cancer. Lancet 2005;365(9472):1727-41.

3. Jemal A, Siegel R, Ward E, et al. Cancer statistics, 2006. CA Cancer J Clin 2006;56(2):106-30.

4. Hanahan D, Weinberg RA. The hallmarks of cancer. Cell 2000;100(1):57-70.

5. Boudreau N, Werb Z, Bissell MJA-b. Suppression of apoptosis by basement membrane requires three-dimensional tissue organization and withdrawal from the cell cycle. Proc Natl Acad Sci U S A 1996;93(8):3509-13.

6. Jones PL, Schmidhauser C, Bissell MJ. Regulation of gene expression and cell function by extracellular matrix. Crit Rev Eukaryot Gene Expr 1993;3(2):137-54.

7. Wiseman BS, Werb Z. Stromal effects on mammary gland development and breast cancer. Science 2002;296(5570):1046-9.

8. Bissell MJ, Radisky D. Putting tumours in context. Nat Rev Cancer 2001;1(1):46-54.

9. Radisky D, Hagios C, Bissell MJ. Tumors are unique organs defined by abnormal signaling and context. Semin Cancer Biol 2001;11(2):87-95.

10. Albini A, Sporn MB. The tumour microenvironment as a target for chemoprevention. Nat Rev Cancer 2007.

11. Dell'aica I, Niero R, Piazza F, et al. Hyperforin blocks neutrophil activation of MMP-9, motility and recruitment,and restrains inflammation-triggered angiogenesis and lung fibrosis. J Pharmacol Exp Ther 2007.

12. Debnath J, Brugge JS. Modelling glandular epithelial cancers in three-dimensional cultures. Nat Rev Cancer 2005;5(9):675-88.

13. Naylor MJ, Li N, Cheung J, et al. Ablation of beta1 integrin in mammary epithelium reveals a key role for integrin in glandular morphogenesis and differentiation. J Cell Biol 2005;171(4):717-28.

14. Slamon DJ, Godolphin W, Jones LA, et al. Studies of the HER-2/neu proto-oncogene in human breast and ovarian cancer. Science 1989;244(4905):707-12.

15. Muthuswamy SK, Li D, Lelievre S, Bissell MJ, Brugge JS. ErbB2, but not ErbB1, reinitiates proliferation and induces luminal repopulation in epithelial acini. Nat Cell Biol 2001;3(9):785-92.

16. Debnath J, Mills KR, Collins NL, Reginato MJ, Muthuswamy SK, Brugge JS. The role of apoptosis in creating and maintaining luminal space within normal and oncogene-expressing mammary acini. Cell 2002;111(1):29-40.

17. Nelson CM, Bissell MJ. Of extracellular matrix, scaffolds, and signaling: tissue architecture regulates development, homeostasis, and cancer. Annu Rev Cell Dev Biol 2006;22:287-309.

18. Bissell MJ, Radisky DC, Rizki A, Weaver VM, Petersen OW. The organizing principle: microenvironmental influences in the normal and malignant breast. Differentiation 2002;70(9-10):537-46.

19. Weaver VM, Petersen OW, Wang F, et al. Reversion of the malignant phenotype of human breast cells in three-dimensional culture and in vivo by integrin blocking antibodies. J Cell Biol 1997;137(1):231-45.

20. Sternlicht MD, Lochter A, Sympson CJ, et al. The stromal proteinase MMP3/stromelysin-1 promotes mammary carcinogenesis. Cell 1999;98(2):137-46.

21. Thomasset N, Lochter A, Sympson CJ, et al. Expression of autoactivated stromelysin-1 in mammary glands of transgenic mice leads to a reactive stroma during early development. Am J Pathol 1998;153(2):457-67.

22. Lochter A, Galosy S, Muschler J, Freedman N, Werb Z, Bissell MJ. Matrix metalloproteinase stromelysin-1 triggers a cascade of molecular alterations that leads to stable epithelial-to-mesenchymal conversion and a premalignant phenotype in mammary epithelial cells. J Cell Biol 1997;139(7):1861-72.

23. Radisky DC, Levy DD, Littlepage LE, et al. Rac1b and reactive oxygen species mediate MMP-3-induced EMT and genomic instability. Nature 2005;436(7047):123-7.

24. Paszek MJ, Zahir N, Johnson KR, et al. Tensional homeostasis and the malignant phenotype. Cancer Cell 2005;8(3):241-54.

25. Ferguson JE, Schor AM, Howell A, Ferguson MW. Tenascin distribution in the normal human breast is altered during the menstrual cycle and in carcinoma. Differentiation 1990;42(3):199-207.

26. Jones PL, Boudreau N, Myers CA, Erickson HP, Bissell MJ. Tenascin-C inhibits extracellular matrix-dependent gene expression in mammary epithelial cells. Localization of active regions using recombinant tenascin fragments. J Cell Sci 1995;108 (Pt 2):519-27.

27. Jahkola T, Toivonen T, Nordling S, von Smitten K, Virtanen I. Expression of tenascin-C in intraductal carcinoma of human breast: relationship to invasion. Eur J Cancer 1998;34(11):1687-92.

28. Mackie EJ, Chiquet-Ehrismann R, Pearson CA, et al. Tenascin is a stromal marker for epithelial malignancy in the mammary gland. Proc Natl Acad Sci U S A 1987;84(13):4621-5.

29. Ishihara A, Yoshida T, Tamaki H, Sakakura T. Tenascin expression in cancer cells and stroma of human breast cancer and its prognostic significance. Clin Cancer Res 1995;1(9):1035-41.

30. Suwiwat S, Ricciardelli C, Tammi R, et al. Expression of extracellular matrix components versican, chondroitin sulfate, tenascin, and hyaluronan, and their association with disease outcome in node-negative breast cancer. Clin Cancer Res 2004;10(7):2491-8.

31. Minn AJ, Gupta GP, Siegel PM, et al. Genes that mediate breast cancer metastasis to lung. Nature 2005;436(7050):518-24.

32. Streuli CH, Bissell MJ. Expression of extracellular matrix components is regulated by substratum. J Cell Biol 1990;110(4):1405-15.

33. Streuli CH, Schmidhauser C, Bailey N, et al. Laminin mediates tissue-specific gene expression in mammary epithelia. J Cell Biol 1995;129(3):591-603.

34. Debnath J, Muthuswamy SK, Brugge JS. Morphogenesis and oncogenesis of MCF-10A mammary epithelial acini grown in three-dimensional basement membrane cultures. Methods 2003;30(3):256-68.

35. Li ML, Aggeler J, Farson DA, Hatier C, Hassell J, Bissell MJ. Influence of a reconstituted basement membrane and its components on casein gene expression and secretion in mouse mammary epithelial cells. Proc Natl Acad Sci U S A 1987;84(1):136-40.

36. Jones PL. Extracellular matrix and tenascin-C in pathogenesis of breast cancer. Lancet 2001;357(9273):1992-4.

37. Jones FS, Jones PL. The tenascin family of ECM glycoproteins: structure, function, and regulation during embryonic development and tissue remodeling. Dev Dyn 2000;218(2):235-59.

38. Orend G, Chiquet-Ehrismann R. Tenascin-C induced signaling in cancer. Cancer Lett 2006.

39. Reginato MJ, Mills KR, Becker EB, et al. Bim regulation of lumen formation in cultured mammary epithelial acini is targeted by oncogenes. Mol Cell Biol 2005;25(11):4591-601.

40. Bissell MJ, Rizki A, Mian IS. Tissue architecture: the ultimate regulator of breast epithelial function. Curr Opin Cell Biol 2003;15(6):753-62.

41. Raser JM, O'Shea EK. Noise in gene expression: origins, consequences, and control. Science 2005;309(5743):2010-3.

42. Zahir N, Weaver VM. Death in the third dimension: apoptosis regulation and tissue architecture. Curr Opin Genet Dev 2004;14(1):71-80.

43. Efron B, Tibshirani R. An Introduction to the bootstrap. New York: Chapman & Hall; 1993.

44. Lengyel E, Prechtel D, Resau JH, et al. C-Met overexpression in node-positive breast cancer identifies patients with poor clinical outcome independent of Her2/neu. Int J Cancer 2005;113(4):678-82.

45. Tsarfaty I, Resau JH, Rulong S, Keydar I, Faletto DL, Vande Woude GF. The met proto-oncogene receptor and lumen formation. Science 1992;257(5074):1258-61.

46. Ghoussoub RA, Dillon DA, D'Aquila T, Rimm EB, Fearon ER, Rimm DL. Expression of c-met is a strong independent prognostic factor in breast carcinoma. Cancer 1998;82(8):1513-20.

47. Camp RL, Rimm EB, Rimm DL. Met expression is associated with poor outcome in patients with axillary lymph node negative breast carcinoma. Cancer 1999;86(11):2259-65.

48. Ioachim E, Charchanti A, Briasoulis E, et al. Immunohistochemical expression of extracellular matrix components tenascin, fibronectin, collagen type IV and laminin in breast cancer: their prognostic value and role in tumour invasion and progression. Eur J Cancer 2002;38(18):2362-70.

49. Howlett AR, Bissell MJ. The influence of tissue microenvironment (stroma and extracellular matrix) on the development and function of mammary epithelium. Epithelial Cell Biol 1993;2(2):79-89.

50. Rizki A, Bissell MJ. Homeostasis in the breast: it takes a village. Cancer Cell 2004;6(1):1-2.

51. Roskelley CD, Bissell MJ. The dominance of the microenvironment in breast and ovarian cancer. Semin Cancer Biol 2002;12(2):97-104.

52. Huang W, Chiquet-Ehrismann R, Moyano JV, Garcia-Pardo A, Orend G. Interference of tenascin-C with syndecan-4 binding to fibronectin blocks cell adhesion and stimulates tumor cell proliferation. Cancer Res 2001;61(23):8586-94.

53. Dandachi N, Hauser-Kronberger C, More E, et al. Co-expression of tenascin-C and vimentin in human breast cancer cells indicates phenotypic transdifferentiation during tumour progression: correlation with histopathological parameters, hormone receptors, and oncoproteins. J Pathol 2001;193(2):181-9.

54. Beiter K, Hiendlmeyer E, Brabletz T, et al. beta-Catenin regulates the expression of tenascin-C in human colorectal tumors. Oncogene 2005;24(55):8200-4.

55. Kobel M, Budianto D, Schmitt WD, Borsi L, Siri A, Hauptmann S. Influence of various cytokines on adhesion and migration of the colorectal adenocarcinoma cell line HRT-18. Oncology 2005;68(1):33-9.

56. Tanaka K, Hiraiwa N, Hashimoto H, Yamazaki Y, Kusakabe M. Tenascin-C regulates angiogenesis in tumor through the regulation of vascular endothelial growth factor expression. Int J Cancer 2004;108(1):31-40.

57. Orend G, Huang W, Olayioye MA, Hynes NE, Chiquet-Ehrismann R. Tenascin-C blocks cell-cycle progression of anchorage-dependent fibroblasts on fibronectin through inhibition of syndecan-4. Oncogene 2003;22(25):3917-26.

58. Tremble P, Chiquet-Ehrismann R, Werb Z. The extracellular matrix ligands fibronectin and tenascin collaborate in regulating collagenase gene expression in fibroblasts. Mol Biol Cell 1994;5(4):439-53.

59. Swindle CS, Tran KT, Johnson TD, et al. Epidermal growth factor (EGF)-like repeats of human tenascin-C as ligands for EGF receptor. J Cell Biol 2001;154(2):459-68.

60. Zukiel R, Nowak S, Wyszko E, et al. Suppression of Human Brain Tumor with Interference RNA Specific for Tenascin-C. Cancer Biol Ther 2006;5(8).

61. Reardon DA, Akabani G, Coleman RE, et al. Salvage radioimmunotherapy with murine iodine-131-labeled antitenascin monoclonal antibody 81C6 for patients with recurrent primary and metastatic malignant brain tumors: phase II study results. J Clin Oncol 2006;24(1):115-22.

62. Reardon DA, Quinn JA, Akabani G, et al. Novel human IgG2b/murine chimeric antitenascin monoclonal antibody construct radiolabeled with 131I and administered into the surgically created resection cavity of patients with malignant glioma: phase I trial results. J Nucl Med 2006;47(6):912-8.

63. Boskovitz A, Akabani GH, Pegram CN, Bigner DD, Zalutsky MR. Human/murine chimeric 81C6 F(ab')(2) fragment: preclinical evaluation of a potential construct for the targeted radiotherapy of malignant glioma. Nucl Med Biol 2004;31(3):345-55.

64. Rizzieri DA, Akabani G, Zalutsky MR, et al. Phase 1 trial study of 131I-labeled chimeric 81C6 monoclonal antibody for the treatment of patients with non-Hodgkin lymphoma. Blood 2004;104(3):642-8.

65. Hicke BJ, Stephens AW, Gould T, et al. Tumor targeting by an aptamer. J Nucl Med 2006;47(4):668-78.

66. Sarkar S, Nuttall RK, Liu S, Edwards DR, Yong VW. Tenascin-C stimulates glioma cell invasion through matrix metalloproteinase-12. Cancer Res 2006;66(24):11771-80.

67. Werb Z, Ashkenas J, MacAuley A, Wiesen JF. Extracellular matrix remodeling as a regulator of stromal-epithelial interactions during mammary gland development, involution and carcinogenesis. Braz J Med Biol Res 1996;29(9):1087-97.

68. Duffy MJ. Urokinase plasminogen activator and its inhibitor, PAI-1, as prognostic markers in breast cancer: from pilot to level 1 evidence studies. Clin Chem 2002;48(8):1194-7.

69. Jahkola T, Toivonen T, von Smitten K, Virtanen I, Wasenius VM, Blomqvist C. Cathepsin-D, urokinase plasminogen activator and type-1 plasminogen activator inhibitor in early breast cancer: an immunohistochemical study of prognostic value and relations to tenascin-C and other factors. Br J Cancer 1999;80(1-2):167-74.

70. Franz M, Hansen T, Richter P, et al. Complex formation of the laminin-5 gamma2 chain and large unspliced tenascin-C in oral squamous cell carcinoma in vitro and in situ: implications for sequential modulation of extracellular matrix in the invasive tumor front. Histochem Cell Biol 2006;126(1):125-31.

71. Settles DL, Cihak RA, Erickson HP. Tenascin-C expression in dystrophin-related muscular dystrophy. Muscle Nerve 1996;19(2):147-54.

72. Taverna D, Disatnik MH, Rayburn H, et al. Dystrophic muscle in mice chimeric for expression of alpha5 integrin. J Cell Biol 1998;143(3):849-59.

73. Muschler J, Levy D, Boudreau R, Henry M, Campbell K, Bissell MJ. A role for dystroglycan in epithelial polarization: loss of function in breast tumor cells. Cancer Res 2002;62(23):7102-9.

74. Niranjan B, Buluwela L, Yant J, et al. HGF/SF: a potent cytokine for mammary growth, morphogenesis and development. Development 1995;121(9):2897-908.

75. Peruzzi B, Bottaro DP. Targeting the c-Met signaling pathway in cancer. Clin Cancer Res 2006;12(12):3657-60.

76. Beviglia L, Matsumoto K, Lin CS, Ziober BL, Kramer RH. Expression of the c-Met/HGF receptor in human breast carcinoma: correlation with tumor progression. Int J Cancer 1997;74(3):301-9.

77. Welm AL, Kim S, Welm BE, Bishop JM. MET and MYC cooperate in mammary tumorigenesis. Proc Natl Acad Sci U S A 2005;102(12):4324-9.

78. Soriano JV, Pepper MS, Nakamura T, Orci L, Montesano R. Hepatocyte growth factor stimulates extensive development of branching duct-like structures by cloned mammary gland epithelial cells. J Cell Sci 1995;108 (Pt 2):413-30.

79. Osin PP, Anbazhagan R, Bartkova J, Nathan B, Gusterson BA. Breast development gives insights into breast disease. Histopathology 1998;33(3):275-83.

80. Gebb SA, Fox K, Vaughn J, McKean D, Jones PL. Fetal oxygen tension promotes tenascin-C-dependent lung branching morphogenesis. Dev Dyn 2005;234(1):1-10.

81. Ihida-Stansbury K, McKean DM, Gebb SA, et al. Paired-related homeobox gene Prx1 is required for pulmonary vascular development. Circ Res 2004;94(11):1507-14.

82. Jones PL, Crack J, Rabinovitch M. Regulation of tenascin-C, a vascular smooth muscle cell survival factor that interacts with the alpha v beta 3 integrin to promote epidermal growth factor receptor phosphorylation and growth. J Cell Biol 1997;139(1):279-93.

83. Bergstrom JD, Westermark B, Heldin NE. Epidermal growth factor receptor signaling activates met in human anaplastic thyroid carcinoma cells. Exp Cell Res 2000;259(1):293-9.

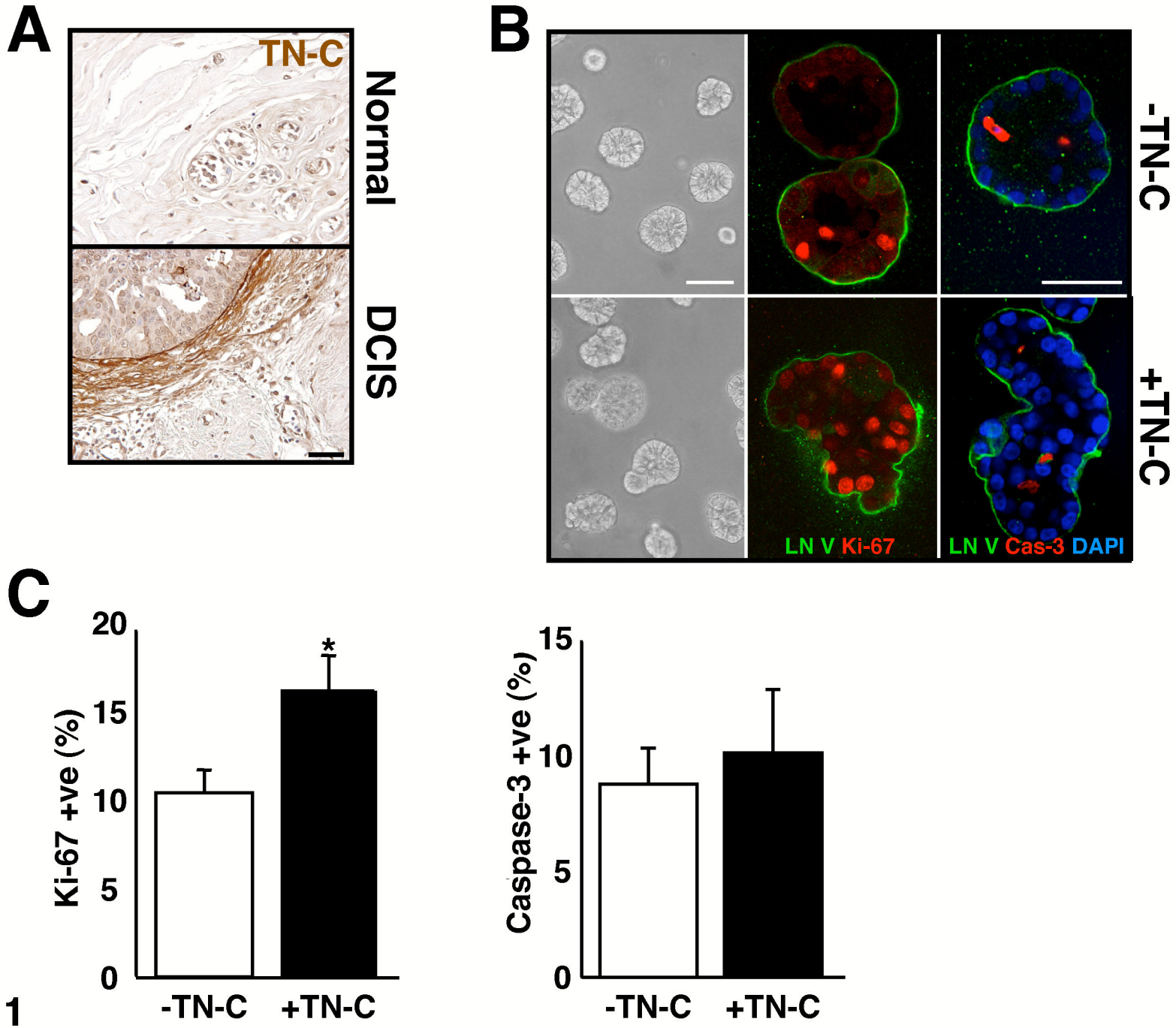
A
TN-C
Normal
DCIS
B
-TN-C
+TN-C
LN V Ki-67
LN V Cas-3 DAPI
C
Ki-67 +ve (%)
20
15
10
5
0
*
-TN-C
+TN-C
Caspase-3 +ve (%)
15
10
5
0
-TN-C
+TN-C

Figure 1

A

Capture 1-2 μm Z-stacks of Laminin V- or α6 integrin-immunostained 3-D acini

↓

Calculate *dx* & *dy* gradient based on fluorescence intensity

↓

Manually initialize active contours & initiate active contour algorithm

↓

Generate 3-D rendition & compare to best-fitting ellipsoid

↓

Calculate acinar surface roughness & volume

B

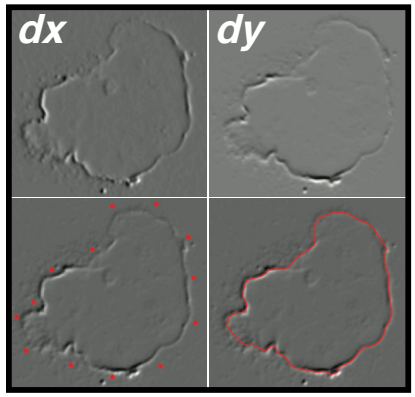

C

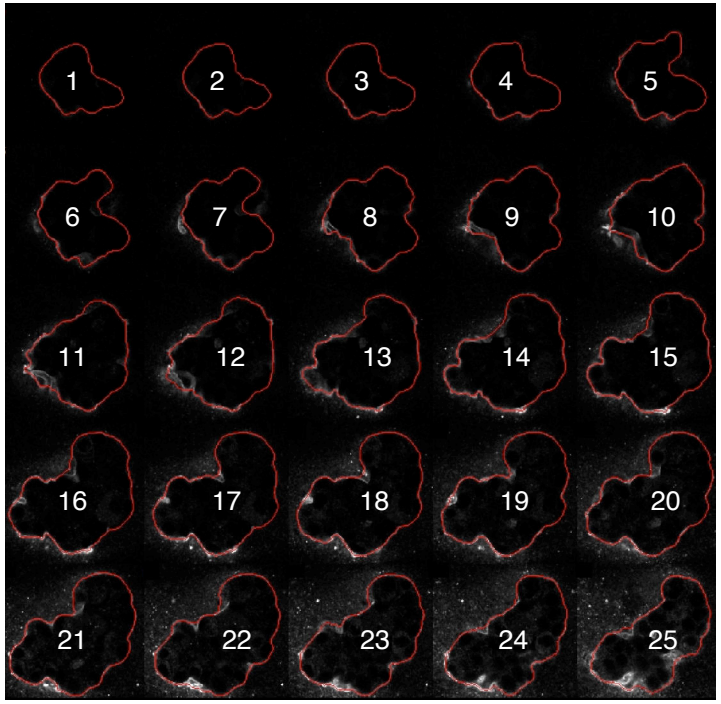

D

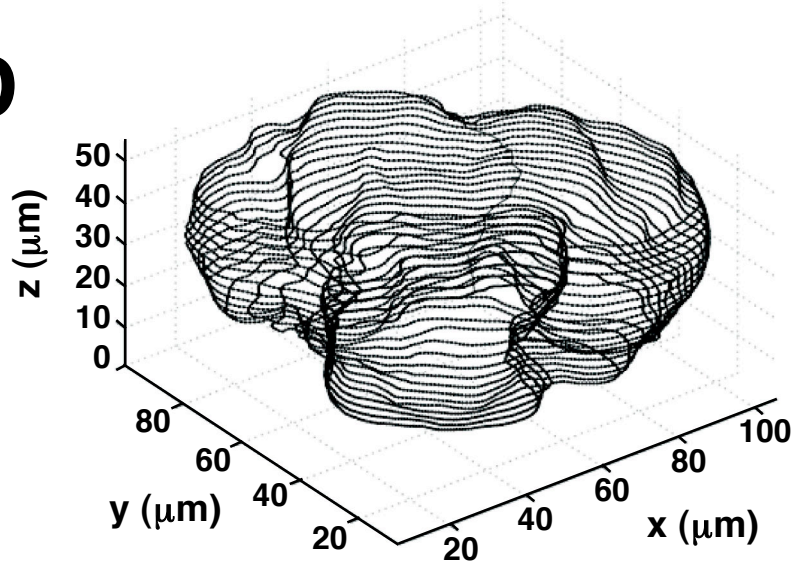

Figure 2

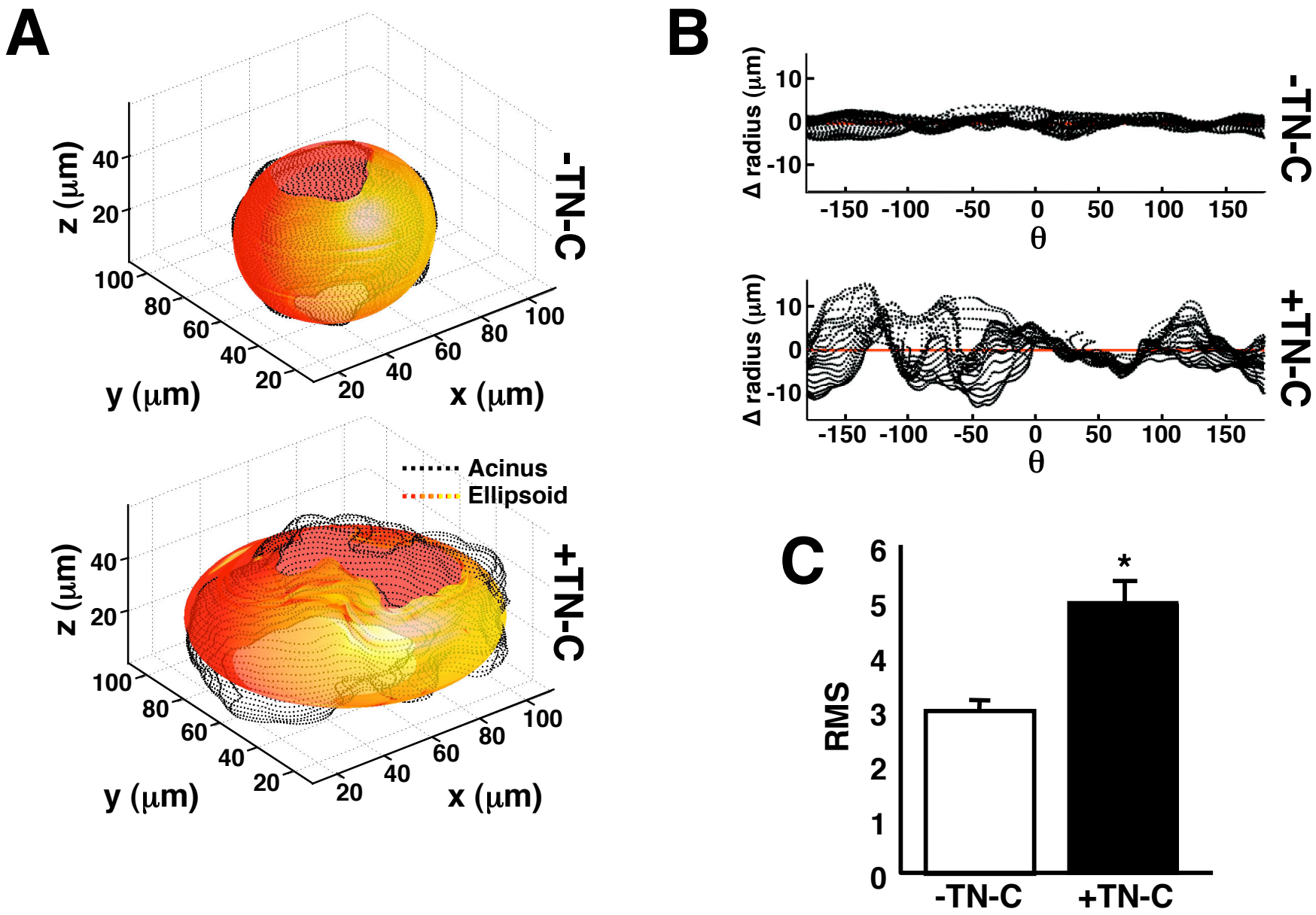

Figure 3

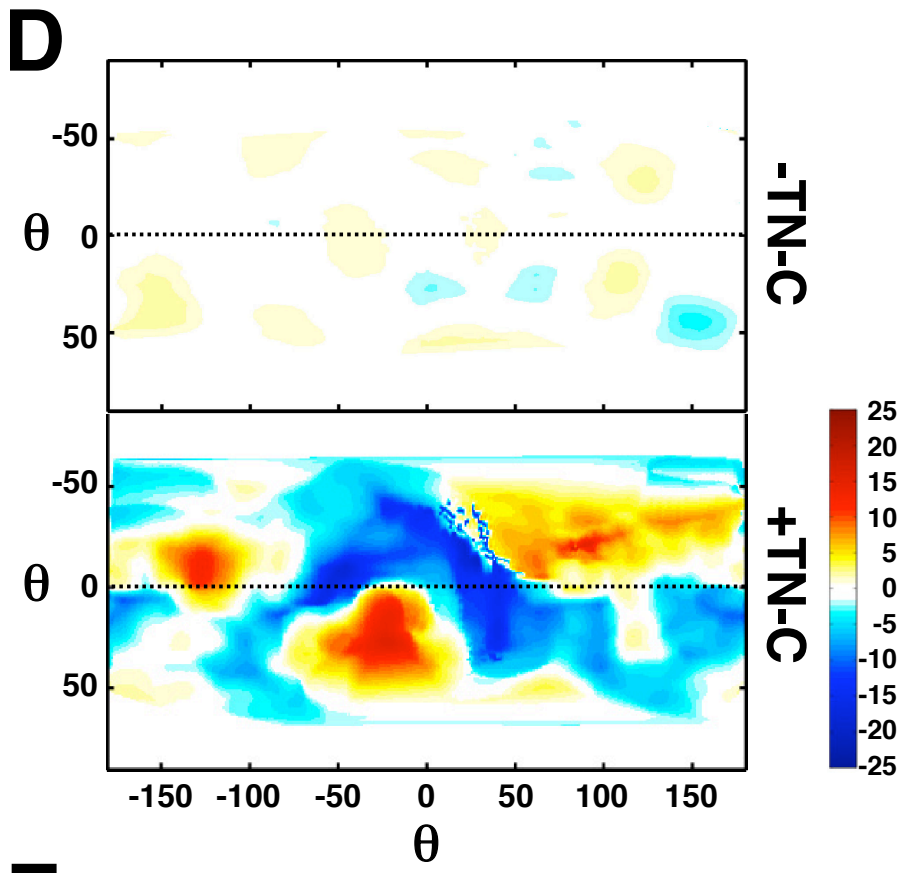

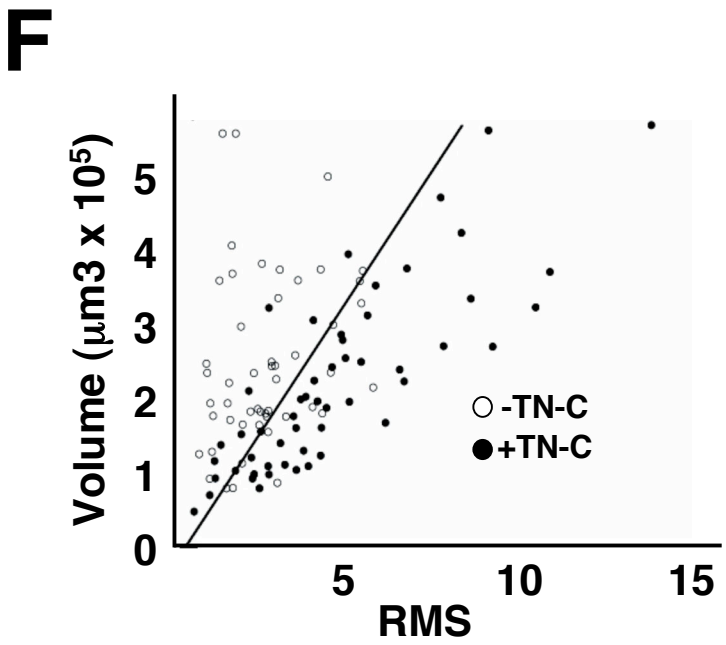

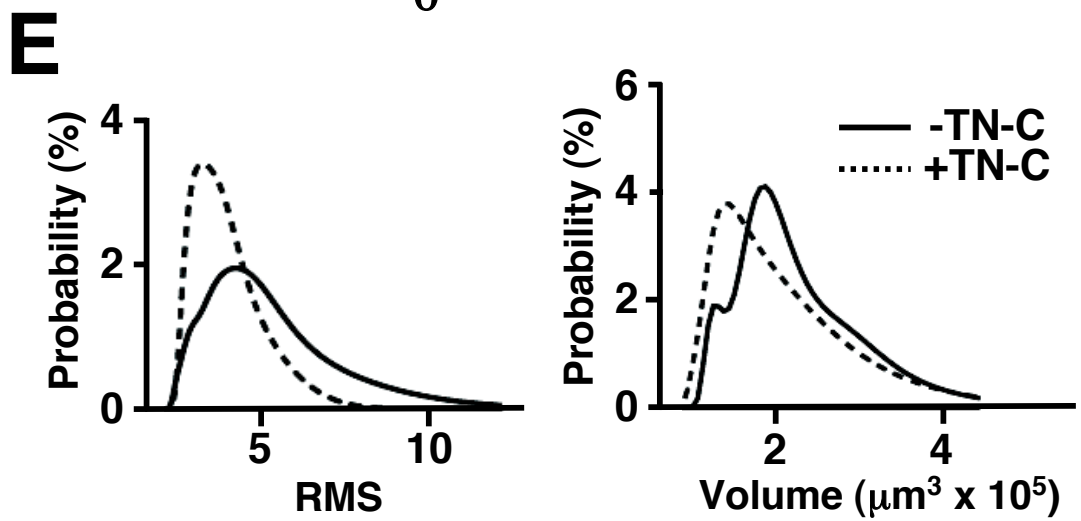

Figure 3 contd

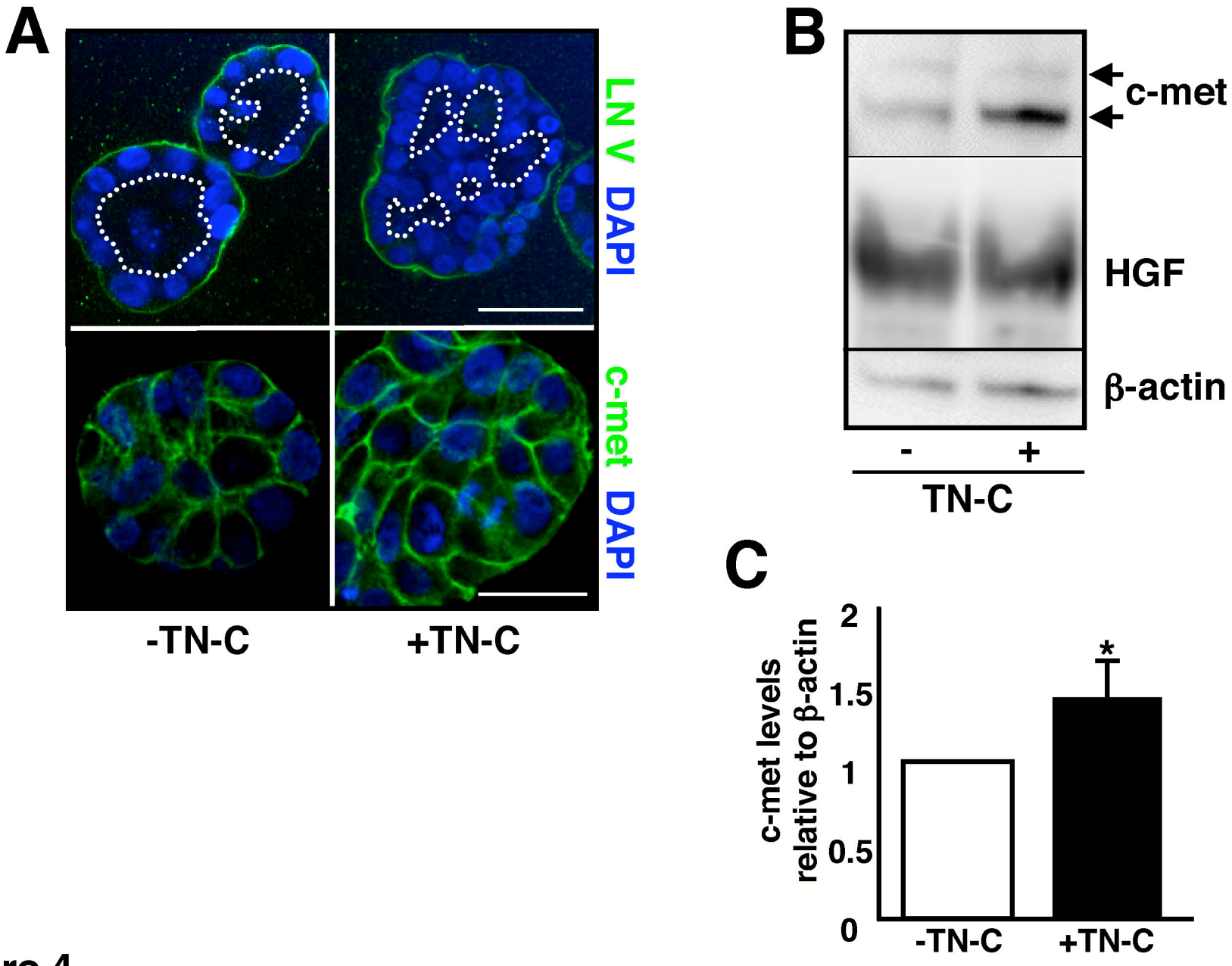
A
LN V DAPI
c-met DAPI
-TN-C
+TN-C
B
c-met
HGF
β-actin
-
+
TN-C
C
c-met levels relative to β-actin
2
1.5
1
0.5
0
*
-TN-C
+TN-C

Figure 4

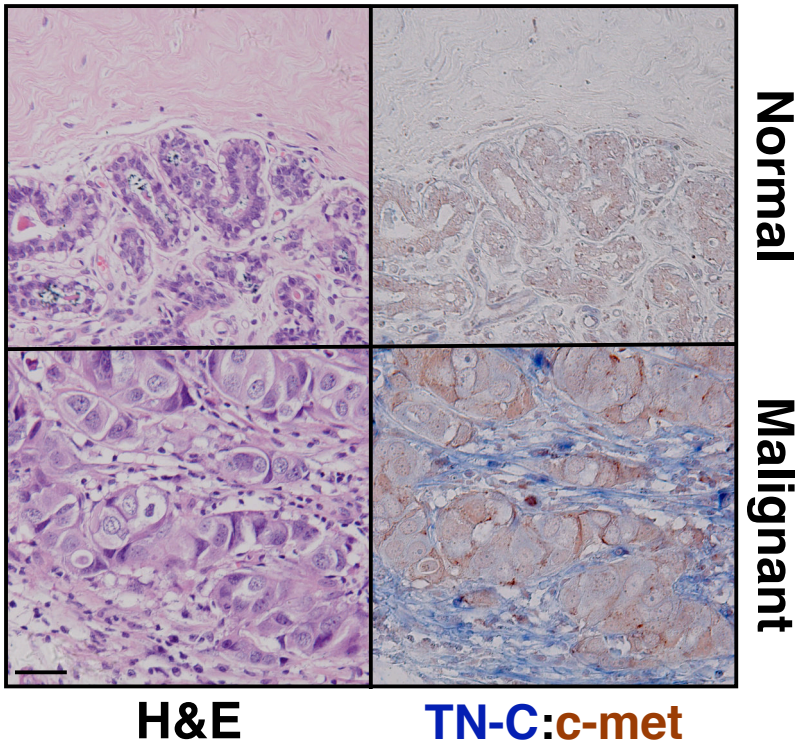

Figure 5

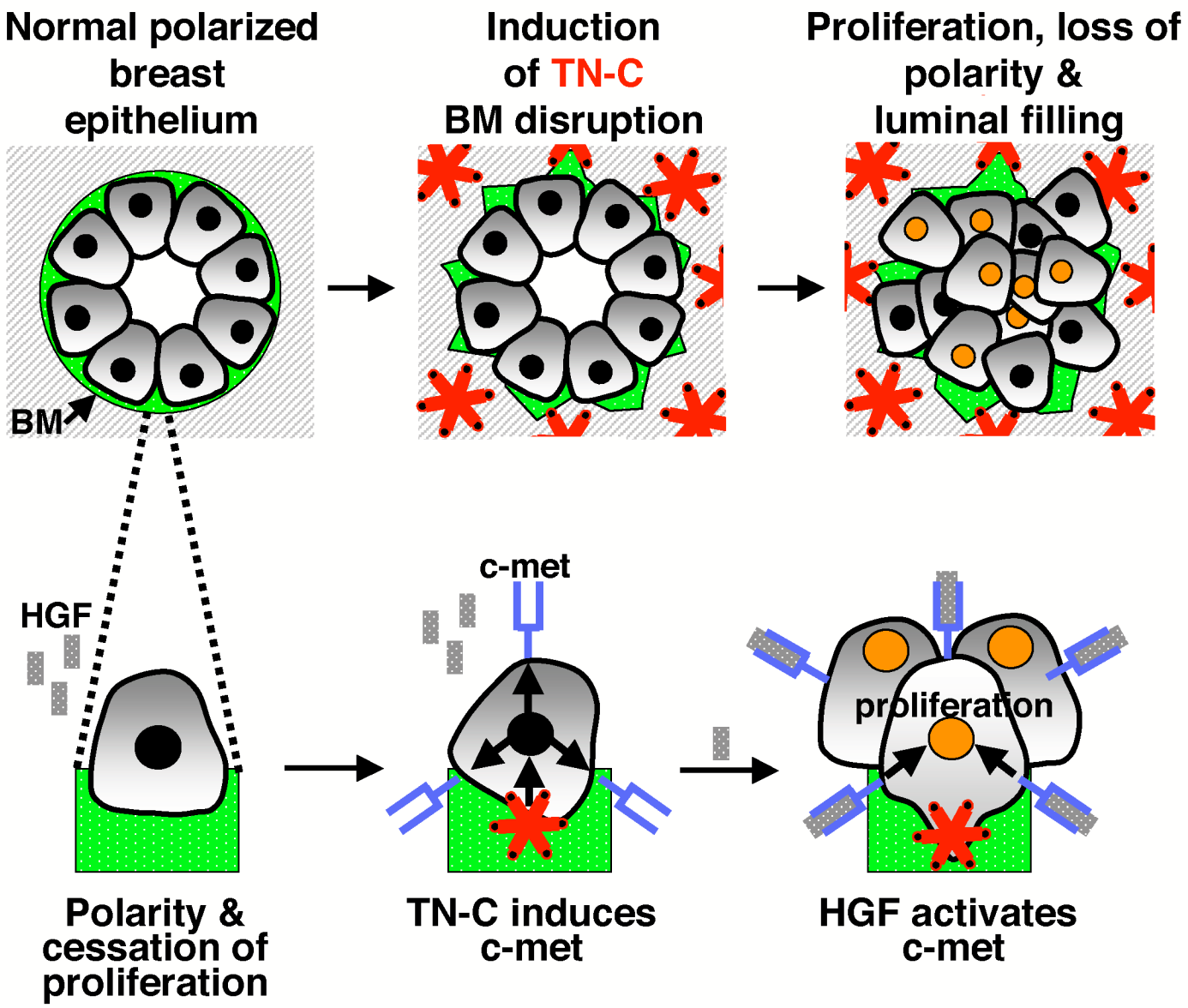
Normal polarized breast epithelium
Induction of TN-C BM disruption
Proliferation, loss of polarity & luminal filling
BM
HGF
c-met
proliferation
Polarity & cessation of proliferation
TN-C induces c-met
HGF activates c-met

Figure 6